A Methodology for Estimating Allocation of Electric Vehicle Grid Interfaces in a Distribution System

Imanthi Kalanika Subasinghe, IEEE Graduate Student member

Real-Time Power and Intelligent Systems Laboratory Holcombe Department of Electrical and Computer Engineering

Clemson University, Clemson, USA.

imanthi@ieee.org

Abstract—The integration of electric vehicles (EVs) into the smart grid has introduced new challenges and opportunities for optimizing power and energy management. This paper presents a simple method using a decision-tree to estimate allocation of vehicle grid interfaces (EVGIs) for charging/discharging, leveraging the nodal capabilities of a distribution system. The future distribution system will cater for vehicle-to-grid (V2G) transactions in addition to grid-to-vehicle (G2V) transactions, thus EVGIs allowing for bidirectional (G2V/V2G) power flows need to be deployed. The proposed decision-tree method is based on nodal power flow ratings and peak demand at the nodes assuming the nodal voltages are maintained within their stability envelopes by volt-var optimization and other voltage control methods. The allocation of EVGIs in the IEEE 34 test node feeder distribution system using the decision-tree method is illustrated. The EVGI allocation using decision-trees is a simple method that can provide insights of a typical distribution system's capability to support EV integration with emerging smart grid technologies.

Keywords—allocation, charging/discharging, distribution system, EV grid interface, nodal power flows.

I. INTRODUCTION

In the quest for achieving net-zero emissions by 2050, the global energy sector is witnessing a remarkable surge in electric vehicle (EV) adoption worldwide. This shift is pivotal in aligning with the goal of limiting the global temperature increase to 1.5°C, as recommended by the Intergovernmental Panel on Climate Change. From 2010 to 2023, the growth trajectory of EV sales has been staggering. By 2022, over 26 million electric cars were on the roads, marking a remarkable increase compared to the previous years as stated in [1]. This trend is set to continue, as depicted in [2].

In recent years, the smart grid concept has emerged [3], reshaping the role of EVs through the development of Vehicle-to-Grid (V2G) technology. V2G facilitates bidirectional energy exchange between electric vehicles and the power grid [4], offering a multitude of services to enhance grid reliability and efficiency [5]. These services include power grid regulation, spinning reserve, peak load shaving, load leveling, and reactive power compensation [6]. Given the complexity of implementing V2G technology, which involves addressing a multifaceted unit commitment problem with conflicting objectives and constraints, optimization techniques become essential.

Ganesh K. Venayagamoorthy, IEEE Fellow
Real-Time Power and Intelligent Systems Laboratory
Holcombe Department of Electrical and
Computer Engineering
Clemson University, Clemson, USA.
Department of Electrical, Electronic and Computer
Engineering, University of Pretoria, South Africa.
gkumar@ieee.org

As the adoption of EVs continues to surge, it is imperative that the current distribution systems adapt to accommodate bidirectional power flow technologies required for Grid-to-Vehicle (G2V) and V2G transactions. This evolution is essential to meet the growing demand for EVs and ensure their seamless integration into the energy ecosystem. Electric vehicle charging infrastructure, represented by charging stations, plays a crucial role in recharging EV batteries. However, the placement of these charging stations cannot be arbitrary [7]. To mitigate the adverse effects associated with EVs, it's essential to undertake optimal planning for sizing and placement. Charging stations can be broadly categorized into slow charging stations (SCS) and rapid charging stations (RCS). In determining the ideal placement and size of charging stations, which hinges on charging demand, established models from transportation modeling literature are commonly employed. The literature reviewed can be categorized into node-based, flow-based, and agent-based approaches [8]. The objectives of infrastructure location models discussed in [9] can be categorized into two main goals: minimizing the cost of charging infrastructure while maintaining a certain level of service, or maximizing the service provided within a given budget.

EV charging station (EVCS) allocation for charging/discharging (C/D) in a distribution system is proposed in [11]. Optimal planning of peak shaving, valley filling and flattening the load curves with EVs is investigated. A multi-objective particle swarm optimization algorithm and the Monte Carlo simulation were applied. To enhance the utilization rates of EV batteries and C/D piles (C/D station), a vehicle-pile resource allocation method was proposed in [12]. This method is based on a two-stage categorical hierarchical scheduling framework designed to address the vehicle-pile assignment problem in near real-time. An optimization model for the joint deployment of EV charging stations and distributed generation resources, considering the V2G function of EVs, is presented in [13].

The contribution of this study is the development of a simple method for estimating the allocation of EV grid interfaces (EVGIs) in distribution systems based on a decision-tree method. The decision-tree method provides the potential locations and the number of EVGIs for any distribution system without any infrastructure upgrade. The EVGI allocation is based on existing capabilities of the distribution system. As future distribution systems are expected to accommodate V2G transactions alongside G2V

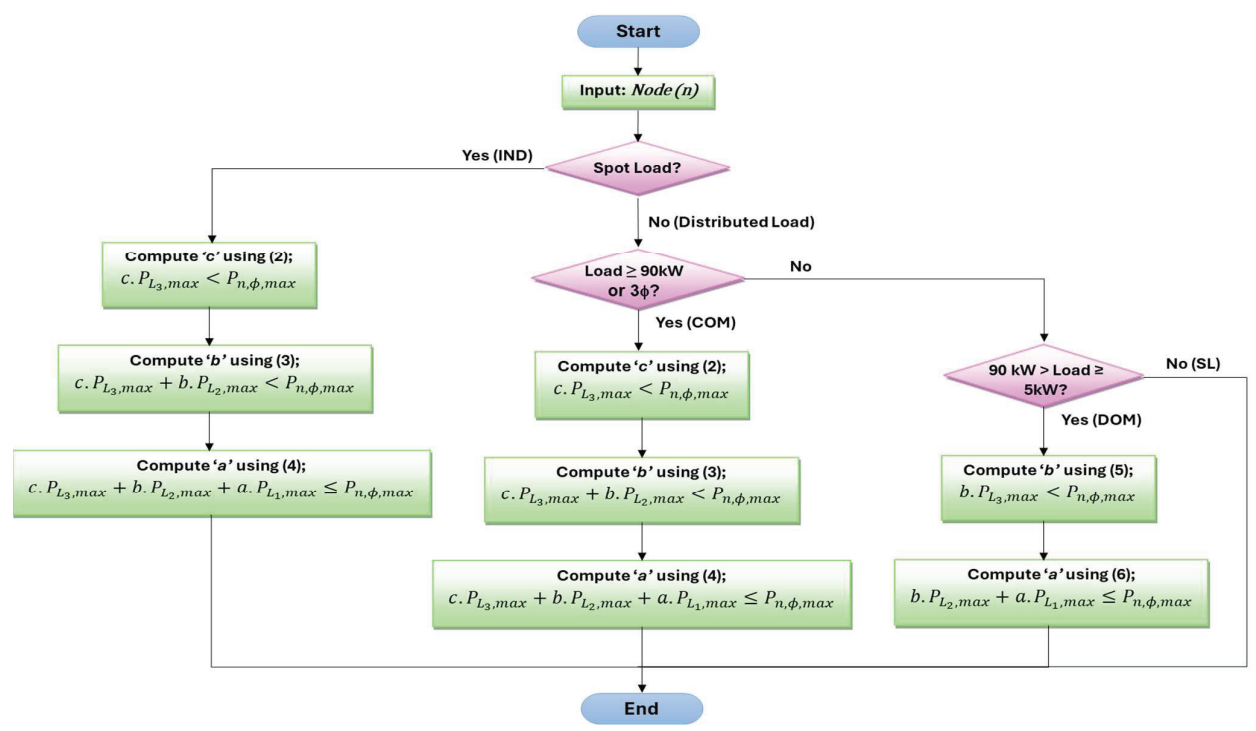


Fig. 1. A decision-tree based methodology for estimating the allocation of EVGIs in a distribution system

transactions, EVGIs capable of bidirectional power flows need be installed. The proposed method relies on nodal power flow ratings and peak demand at the nodes, while assuming that nodal voltages remain within their designated envelopes with or without volt-var optimization. Furthermore, the proposed decision-tree method for EVGI allocation that can be used for any given distribution system, based on the objectives, which provides a node-based model to minimize the cost while maximizing the level of service. The G2V demand can be decided according to the difference between the peak and the current load demands while, the load is dynamically changing in a 24 hour window.

The rest of the paper is as follows; Section II describes the problem formulation for EVGI allocation. Section III illustrates the decision-tree methodology applied to the IEEE 34 bus feeder system. Section IV presents typical results and discussions on the allocation of EVGIs. Finally, the conclusion is given in Section V.

II. PROBLEM FORMULATION

Scaling up the EVGI allocation in a specific distribution system involves several assumptions. The allocation is based on the system infrastructure ratings, which includes factors such as the number of nodes, phases, and types of dynamic loads connected. In the proposed method aimed at EVGI allocation estimation, the following basic assumptions are considered:

- Discharging levels are functionally analogous to charging levels with bidirectional inverter capabilities.
- Discharge rate is within the safe envelope for the batteries as in the case of charging.
- Allocation of the grid infrastructure is to maximize the charging with capabilities for discharging.

The EVGI allocation is solely depends on the nodal rated power described by (1), where ϕ represents the phase (1, 2, 3), n denotes the node number and a, b, c indicates the number of charging station levels L_j , where j = 1, 2, 3 respectively, for the node. L_1 and L_2 are types of AC charging and L_3 can accommodate the DC fast charging (DCFC) and extreme fast charging (XFC). Therefore, the number of L_3 stations, c can be divided into two namely C_{DCFC} and C_{XFC} representing number of L_3 , DCFCs and XFCs [19]-[23]. To ensure system voltage stability, the maximum power supplied for a phase must not be surpassed. In this study, the maximum G2V/V2G demand per phase in the network is considered fixed according to the dynamics of the nodal load curve, and the system node voltages are assumed to operate within a range of $1.00 \pm 5\%$ p.u. The flowchart in Fig. 1 describes the generalized methodology for the allocation of EVGI based on (1) with the identification of the load type of any given node prioritizing the L_3 and followed by L_2 and L_1 for maximizing the charging capabilities.

$$P_{n,\phi,max} \ge a.P_{L_1,max} + b.P_{L_2,max} + c.P_{L_3,max}$$
 (1)

For the industrial (IND) and commercial (COM) loads, c is computed using (2), and b and a are calculated according to (3) and (4), respectively.

$$c = round\left(\frac{P_{n,\phi,max}}{P_{L_x,max}}\right) \tag{2}$$

to (3) and (4), respectively.
$$c = round \left(\frac{P_{n,\phi,max}}{P_{L_3,max}}\right) \tag{2}$$
 If $c. P_{L_3,max} < P_{n,\phi,max}$, then
$$b = round \left(\frac{P_{n,\phi,max} - c.P_{L_3,max}}{P_{L_2,max}}\right) \tag{3}$$
 If $c. P_{L_3,max} + b. P_{L_2,max} < P_{n,\phi,max}$, then
$$a = round \left(\frac{P_{n,\phi,max} - c.P_{L_3,max} - b.P_{L_2,max}}{P_{L_1,max}}\right) \tag{4}$$
 and $c. P_{L_3,max} + b. P_{L_2,max} + a. P_{L_1,max} \le P_{n,\phi,max}$ should not be violated.

$$a = round\left(\frac{P_{n,\phi,max} - c.P_{L_3,max} - b.P_{L_2,max}}{P_{L_1,max}}\right) \tag{4}$$

not be violated.

Assuming the domestic (DOM) nodes only accommodate

 L_2 and L_1 , b and a are computed using (5) and (6), respectively.

$$b = round\left(\frac{P_{n,\phi,max}}{P_{L_2,max}}\right) \tag{5}$$

$$b = round\left(\frac{P_{n,\phi,max}}{P_{L_2,max}}\right)$$
If $b. P_{L_2,max} < P_{n,\phi,max}$, then
$$a = round\left(\frac{P_{n,\phi,max} - b.P_{L_2,max}}{P_{L_1,max}}\right)$$
and $b. P_{L_2,max} + a. P_{L_1,max} \le P_{n,\phi,max}$ should not be

should

The estimated G2V/V2G demand for the network will depend on the maximum hosting capacity per phase in the network as described by (1). The G2V/V2G transaction for a given node (n) within the system can be explained by (7)where, the total G2V/V2G power at time t, denoted as $P_{n,V2G}$ (t), the load at that moment, represented as $D_n(t)$, the charging demand as $P_{n,G2V}(t)$, the surplus power outflow denoted as $P_{n,out}(t)$ and the drawing power from the grid, $P_{n,in}(t)$. Fig. 2 depicts a nodal's power inflows and outflows corresponding to these scenarios where the $P_{n,max}$ is the maximum power rating in kW of the node and $V_{n,rated}$ is the rated voltage in kV of the n^{th} node.

$$P_{n,V2G}(t) = D_n(t) + P_{n,G2V}(t) + P_{n,out}(t) - P_{n,in}(t)$$
 (7)

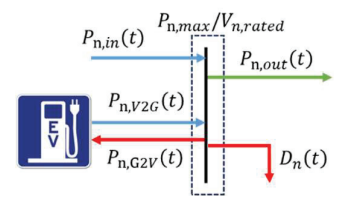


Fig. 2. Nodal power ratings, voltage rating and flow representation.

III. MODIFIED IEEE 34 TEST SYSTEM

The test system for this study is the IEEE 34 test node feeder system illustrated in Fig. 3, represents an actual feeder in Arizona has features reflecting the physical world [1]. The configuration details of the IEEE 34 test node feeder can be accessed by [10] with overhead line configurations, line segment data, transformer data, load data; spot loads, distributed loads, shunt capacitors, regulator data, impedances, power flow results, voltage profiles, power flow data. The 24kV test feeder extends over a considerable distance [5], spanning approximately 36 miles from node 848 to the substation. Despite its length, the feeder experiences low levels of electrical load.

Additionally, the circuit incorporates two voltage line regulators, positioned between nodes 814-850 and 852-832, respectively. Though the published IEEE 34 test node feeder is discussing a radial distribution system with constant kW and kVAr (PQ), constant impedance (Z) and, constant current (I) [9], the teat feeder used in this study has been modified with dynamic loadings of the nodes without violating their ratings for the intention of integrating the EV discharging levels.

A. Static Loads into Daily Dynamic Loads

First the 34 test nodes are categorized into three types of loads: domestic (DOM), industrial (IND) and commercial (COM) [5]. All the spot loads were assumed to be industrial loads. If the loads are single phase and relatively small, less than 5 kW, they are not allocated for the three main categories and assumed as street light (SL) load profiles in the system. Other loads were assumed to be DOM or COM. If they are

less than 90 kW (DOM) and higher than 90 kW (COM) respectively [15]. Table A. I describes the load categorization where the darker orange colored portion is the IND, the medium orange colored is the COM and the mild orange colored is the DOM loads with respect to their phases.

The dynamic load variation of the IEEE 34 test feeder is modeled based on the daily load data provided in [17], which presents dynamic load profiles for 24 hours per day of Southern California Edison. These profiles depict the daily load variations for different types of loads: Industrial (IND), Commercial (COM), and Residential (DOM). Weekday and weekend load profiles exhibit similar shapes with varying peaks throughout the 24-hour period [17]. To reflect these profiles, load data from Southern California Edison has been normalized according to load types (IND, COM, and DOM).

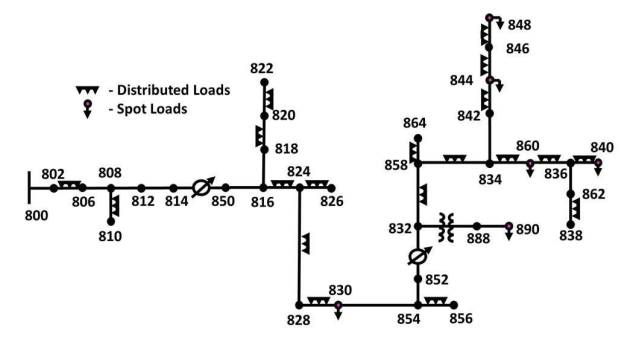


Fig. 3. Types of loads in the radial IEEE 34 test node feeder.

The predefined static nodal load values from guidelines [10] are utilized as the peak loads for dynamic nodal load representation. The dynamic load profiles for the test system are then generated using the normalized load factors for the three load categories. Fig. 5 illustrates the dynamic load variation over 24 hours for example IND, COM, and DOM nodes in the IEEE 34 test feeder as assumed in Table A.I.

B. EV Grid Interface Allocation

In accordance with the assumptions detailed in Section II, the IEEE 34 test node feeder has been enhanced to include, L_1 , L_2 , and , L_3 C/D stations, with the primary objective being the reduction of charging times. Grid infrastructure provides the bidirectional power flow including charging and discharging. The priority for the allocation of EVGI is given to L_3 and followed by L_2 and L_1 .

TABLE I. EVGI TYPES AND RATINGS

EVGI Type	Voltage (V)	Current (A)	Maximum Power Output (kW)		
Level 1	120	12-16 AC/1¢	1.44		
Level 2	208-240	12-80 AC/2¢	6.7-19		
Level 3	400-800	350 DC	50-350		

 L_1 and L_2 stations are assumed to support bidirectional power flow, encompassing both V2G and G2V capabilities. In contrast, L_3 is presumed to be capable solely of G2V at its ratings due to EV battery safety considerations. Consequently, the L_1 , L_2 stations can operate either as G2V or V2G at any given time, allowing unoccupied G2V stations to facilitate V2G operations. The power levels for the specified C/D levels are considered as 1 kW, 19 kW for L_1 and L_2 . L_3 is charging at 50 kW and discharging and 19 kW rates as described in [19-23] and Table 1. The L_3 is assumed to be discharging at the L_2

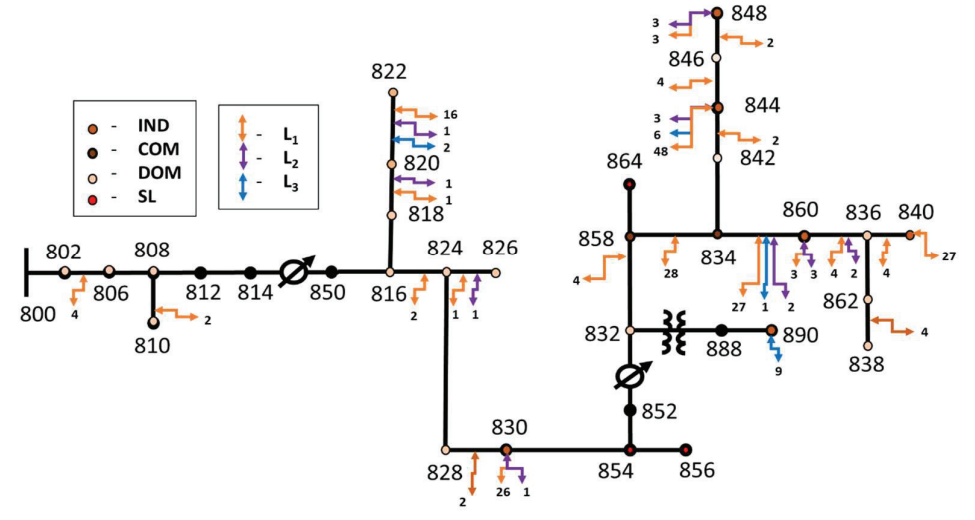


Fig. 4. IEEE 34 test node feeder with allocated EVGIs.

rate. The predefined load parameters outlined in [8] have been adopted as the load constraints for the modified IEEE 34 test node feeder. It is assumed that DOM loads can only support L_1 and L_2 stations and a maximum of two to three EVs, whereas COM and IND loads occupy all charging levels.

IV. RESULTS AND DISCUSSIONS

Consequently, the integration of EVGI stations per phase $(\phi: I, 2, 3)$ for the test system is detailed in Table A.I, IND loads encompass a total of 129 EVGIs, comprising 104 L_{I} s, 10 L_{2} s, and 15 L_{3} s, while DOM hosts 38 EVGIs consisting of 34 L_{I} s and 4 L_{2} s. COM incorporates 34 EVGIs in total, including 71 L1s, 2 L_{2} s, and 4 L_{3} s. Consequently, the modified IEEE 34 distribution system accommodates a total of 206 EVGIs, comprising 175 L_{I} s, 12 L_{2} s, and 19 L_{3} s. The total EVGI allocation is visualized in the Fig. 4, indicating the different charging levels according to the C/D rates.

Illustrated in Fig. 6, which delineates the calculated possible theoretical load profiles: $D_n(t)$, $P_{n,V2G}(t)$, $P_{n,G2V}(t)$, of node 890_1, according to Table A.I. The C/D capacity for electric vehicles (EVs) at each station varies owing to the connected load, as specified in (2). During periods of peak load, G2V charging is assumed to be inactive, whereas the highest demand for G2V charging occurs during intervals of minimum load connected to the node. Therefore, the daily V2G capability for a specific node will be determined by the power rating of the node and the G2V demand (load + G2V) of the node. Fig. 7 describes the practical scenario of the P_{V2G} for the IND node 890,1 which accommodates 3 EVGIs of level 3 with a discharging rate of 19 kW.

V. CONCLUSION

The increasing number of electric vehicles and their integration into distribution systems is becoming a challenge task. This paper has presented the development of a simple method based on decision-tree for determining the potential locations and number of EV grid interfaces in any distribution system. The decision-tree method can be applied based on current nodal peak demand and power flow ratings. Typical results of EVGI allocation have been illustrated for the IEEE 34 node test feeder system. The decision-tree method for the EVGI allocation does not take into consideration accessibility factors, and regulatory and financial factors. Further

validation and refinement are needed due to the unavailability of real-world V2G demand data. Future work includes the estimation and forecasting the V2G demand using intelligent methods and taking into consideration factors affecting the EVGI allocation into the decision-tree, such as accessibility, regulatory and financial/cost, and a methodology for the operational management of the EVGIs.

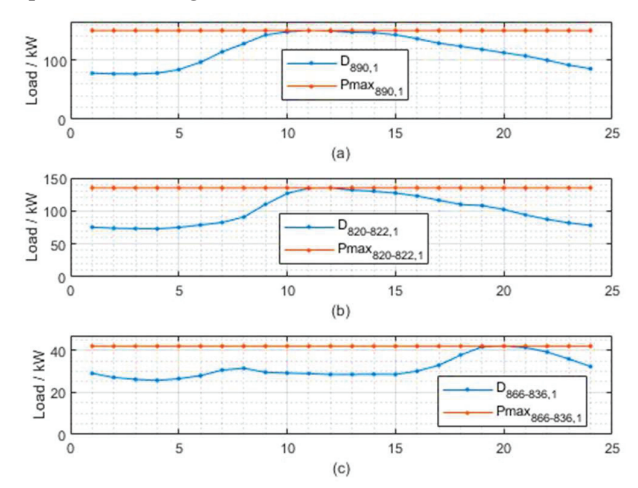


Fig. 5. (a) Daily load curve of IND 890,1; (b) Daily load curve of COM 820-822,1; (c) Daily load curve of DOM 860-836,1.

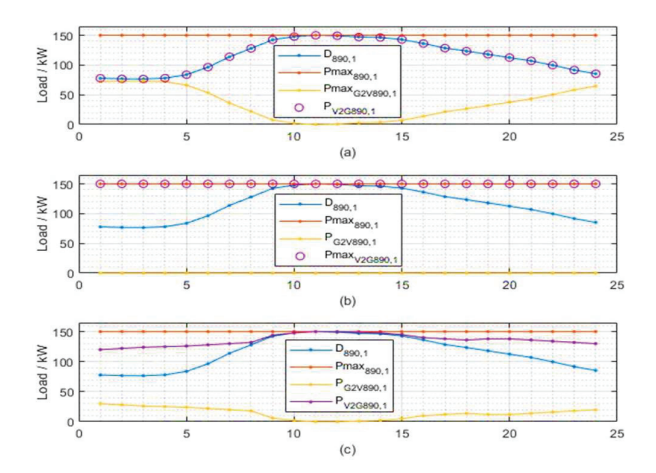


Fig. 6. (a) Maximum possible P_{G2V} ; (b) Maximum possible theoretical P_{V2G} ; (d) Relationship of D_n , P_{G2V} and P_{V2G} .

2024 IEEE PES/IAS PowerAfrica

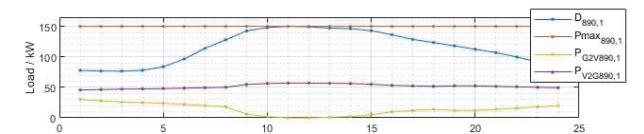


Fig. 7. Maximum possible theoretical P_{V2G} with D_n and P_{G2V} .

REFERENCES

- [1] IEA (2023), Global EV Outlook 2023, IEA, Paris https://www.iea.org/reports/global-ev-outlook-2023, License: CC BY 4.0
- [2] BloombergNEF (2023), Electric Vehicle Outlook 2023 https://about.bnef.com/electric-vehicle-outlook
- [3] H. Kikusato, "Electric Vehicle Charge—Discharge Management for Utilization of Photovoltaic by Coordination Between Home and Grid Energy Management Systems," in IEEE Transactions on Smart Grid, vol. 10, no. 3, pp. 3186-3197, May 2019, doi: 10.1109/TSG.2018.2820026.
- [4] K. Clement-Nyns, E. Haesen, J. Driesen, "The impact of vehicle-to-grid on the distribution grid", Electric Power Systems Research, vol. 81, no. 1, pp 185-192, ISSN 0378-7796, , 2011, https://doi.org/10.1016/j.epsr.2010.08.007.
- [5] S. Huang, W. Liu, J. Zhang, C. Liu, H. Sun, Q. Liao, "Vehicle-to-grid workplace discharging economics as a function of driving distance and type of electric vehicle", Sustainable Energy, Grids and Networks, vol. 31, 100779, ISSN 2352-4677, 2022, https://doi.org/10.1016/j.segan.2022.100779.
- [6] Y. Ma, T. Houghton, A. Cruden, D. Infield, "Modeling the Benefits of Vehicle-to-Grid Technology to a Power System," in IEEE Transactions on Power Systems, vol. 27, no. 2, pp. 1012-1020, May 2012, doi: 10.1109/TPWRS.2011.2178043.
- [7] R. S. Gupta, A.Tyagi, S. Anand. "Optimal allocation of electric vehicles charging infrastructure, policies and future trends." Journal of Energy Storage 43, pp 103291, 2022.
- [8] T. Unterluggauer, J. Rich, P. B. Andersen, S. Hashemi. "Electric vehicle charging infrastructure planning for integrated transportation and power distribution networks: A review." ETransportation, pp 12: 100163, 2022.
- [9] W. H. Kersting, "Radial distribution test feeders," in IEEE Transactions on Power Systems, vol. 6, no. 3, pp. 975-985, Aug. 1991, doi: 10.1109/59.119237.
- [10] Radial Test Feeders IEEE Distribution System Analysis Subcommittee; [Online]. Available: http://www.ewh.ieee.org/soc/pes/dsacom/testfeeders.html
- [11] E. Hadian, H. Akbari, M. Farzinfar and S. Saeed, "Optimal Allocation of Electric Vehicle Charging Stations With Adopted Smart Charging/Discharging Schedule," in IEEE Access, vol. 8, pp. 196908-196919, 2020, doi: 10.1109/ACCESS.2020.3033662.
- [12] J. Xu, Y. Huang. "The short-term optimal resource allocation approach for electric vehicles and V2G service stations." Applied Energy, pp 319: 119200, 2022.
- [13] L. Luo, Z. Wu., W. Gu, H. Huang, S. Gaoand, J. Han, "Coordinated allocation of distributed generation resources and electric vehicle charging stations in distribution systems with vehicle-to-grid interactio", Energy, 192, pp.116631, 2020.
- [14] A. J. O. Owuor, J. L. Munda and A. A. Jimoh, "The ieee 34 node radial test feeder as a simulation testbench for Distributed Generation," IEEE Africon '11, Victoria Falls, Zambia, 2011, pp. 1-6, doi: 10.1109/AFRCON.2011.6072095.
- [15] B. A. Mather, "Quasi-static time-series test feeder for PV integration analysis on distribution systems," 2012 IEEE Power and Energy Society General Meeting, San Diego, CA, USA, 2012, pp. 1-8, doi: 10.1109/PESGM.2012.6345414.
- [16] K. M. Tan, V. K. Ramachandaramurthy, J. Y. Yong, , "Integration of electric vehicles in smart grid: A review on vehicle to grid technologies and optimization techniques," Renewable and Sustainable Energy Reviews, Elsevier, vol. 53©, pp 720-732, 2016.

- [17] Southern California Edison, 2023 Dynamic Load Profiles, online resource: https://www.sce.com/regulatory/load-profiles/dynamic-load-profiles
- [18] Northwest Power and Conservation Council, Plug-In Electric Load Profiles, online source: https://www.nwcouncil.org/2021powerplan_plug-electric-load-profiles/
- [19] S. Palanisamy, S. Chenniappan, S. Padmanaban, "Distribution System Planning in Fast-Charging Infrastructure for Electric and Hybrid Electric Vehicles: Methods for Large-Scale Penetration into Electric Distribution Networks", IEEE, 2023, pp.59-81, doi: 10.1002/9781119987772.ch11.
- [20] IEC 61851-1:2017(2017). Electric vehicle conductive charging system- Part 1: General requirements. 12-15 IEC Standards.
- [21] EPRI, Plug-In Electric Vehicle Infrastructure Installation Guidelines, Sep 25, 2009, US.
- [22] https://www.transportation.gov/rural/ev/toolkit/ev-basics/chargingspeeds
- [23] Powar, Vishwas, and Rajendra Singh, "End-to-End Direct-Current-Based Extreme Fast Electric Vehicle Charging Infrastructure Using Lithium-Ion Battery Storage" Batteries 9, no. 3: 169, 2023. https://doi.org/10.3390/batteries9030169
- [24] G. K. Venayagamoorthy, R. K. Sharma, P. K. Gautam and A. Ahmadi, "Dynamic Energy Management System for a Smart Microgrid," in IEEE Transactions on Neural Networks and Learning Systems, vol. 27, no. 8, pp. 1643-1656, Aug. 2016, doi: 10.1109/TNNLS.2016.2514358.
- [25] A. Pal, A. Bhattacharya, A. K. Chakraborty. "Allocation of electric vehicle charging station considering uncertainties." Sustainable Energy, Grids and Networks, pp 25: 100422, 2021.

VI. APPENDIX

TABLE A. I ALLOCATED OF EVGI FOR THE IEEE 34 TEST NODE

п,ф \			L1		1.2		1.3		
	Vrated (kV)	Pmax (kW)	C/D Rating (kW)	Num. of L1	C/D Rating (kW)	Num. of L2	C Rating (kW)	Num. of L3	D Rating (kW
860,1	24.9	20	1		19	1	50		19
860,2	24.9	20	1		19	1	50		19
860,3	24.9	20	1		19	1	50		19
840,1	24.9	9	1	9	19		50		19
840,2	24.9	9	1	9	19		50	-	19
840,3	24.9	9	1	9	19		50	-	19
844,1	24.9	135	1	16	19	1	50	2	19
844,2	24.9	135	1	16	19	1	50	2	19
844,3	24.9	135	1	16	19	1	50	2	19
848,1	24.9	20	1	1	19	1	50		19
848,2	24.9	20	1	1	19	1	50		19
848,3	24.9	20	1	1	19	1	50		19
890,1	4.16	150	1		19	-	50	3	19
890,2	4.16	150	1	-	19		50	3	19
890,3	4.16	150	1		19	-	50	3	19
830,1	24.9	10	1	10	19		50		19
830,2	24.9	10	1	10	19		50		19
830,3	24.9	2.5	1	6	19	1	50		19
820-822,1	24.9	135	1	16	19	1	50	2	19
858-834,2	24.9	15	1	15	19		50		19
858-834.3	24.9	13	1	13	19		50		19
834-860,1	24.9	16	1	16	19	-	50		19
834-860,2	24.9	20	1	1	19	1	50		19
834-860,3	24.9	110	1	10	19		50	2	19
802-806,2	24.9	30	1	2	19		50		19
802-806,3	24.9	25	1	2	19		50		19
808-810,2	24.9	16	1	2	19		50		19
818-820,1	24.9	34	1	1	19	1	50		19
816-824,2	24.9	5	1	2	19		50		19
824-826,2	24.9	40	1	1	19	1	50		19
828-830,1	24.9	7	1	2	19		50		19
832-858,1	24.9	7	1	2	19		50		19
832-858,3	24.9	6	1	2	19		50		19
860-836,1	24.9	30	1	1	19	1	50	-	19
860-836,2	24.9	10	1	2	19	-	50	-	19
860-836,3	24.9	42	1	1	19	1	50	-	19
836-840,1	24.9	18	1	2	19	-	50		19
836-840,2	24.9	22	1	2	19	-	50	-	19
862-838,2	24.9	28	1	2	19	-	50	-	19
842-844,1	24.9	9	1	2	19		50		19
844-846,2	24.9	25	1	2	19		50		19
844-846,3	24.9	20	1	2	19	-	50	-	19
846-848,2	24.9	23	1	2	19		50		19